PVTx Properties of Gaseous Mixtures of Difluoromethane and 1,1,1,2,3,3,3-Heptafluoropropane

Xiao-Juan Feng, Yuan-Yuan Duan,* and Wei Dong

Key Laboratory for Thermal Science and Power Engineering of MOE, Department of Thermal Engineering,
Tsinghua University, Beijing, 100084, People's Republic of China

---

Mixtures of difluoromethane (HFC-32) and 1,1,1,2,3,3,3-heptafluoropropane (HFC-227ea) are promising alternative refrigerants; however, there is currently no available published experimental *PVTx* data. The gaseous *PVTx* properties of HFC-32 (1) + HFC-227ea (2) mixtures were measured using the Burnett-isochoric method with 251 data sets obtained for temperatures from (310 to 410) K, pressures up to 3658 kPa, and densities up to 206 kg·m^{-3} at $x_1 = 0.2648$, $x_1 = 0.5155$, and $x_1 = 0.7809$. The temperature, pressure, and mole fraction uncertainties were estimated to be ±10 mK, ±100 Pa, and ±0.01 %, respectively. A truncated virial equation was used to correlate the experimental data, with the second and third virial coefficients for the binary mixtures also determined.

Introduction

Mixtures of HFC-32 and HFC-227ea are promising alternative refrigerants to replace chlorodifluoromethane (HFC-22). However, there is only published experimental data for the vapor−liquid equilibrium and the surface tension of such mixtures[1−4] with no gaseous *PVTx* properties reported in the literature until now. We previously repeated[5] precise *PVTx* data for mixtures of difluoromethane (HFC-32) + pentafluoroethane (HFC-125). The present results were obtained with the same experimental system with some improvements. The results include *PVTx* properties for gaseous HFC-32 + HFC-227ea mixtures for three compositions for temperatures from (310 to 410) K.

Experimental Section

The Burnett-isochoric coupling method was used for present measurements. A diagram of the apparatus is shown in Figure 1. The system is similar to that described by Fu et al.[6] with improvements in the pressure measurement system, the vacuum system, and the sampling system. The sample cells were also rebuilt.

The thermostat bath temperature could be varied from (223 to 453) K with an uncertainty of less than ±2 mK in 1 h and less than ±5 mK in 8 h. The temperature range for these experiments was from (310 to 410) K; thus, silicone oil was used as the bath fluid. The temperature measurement system included two platinum resistance thermometers (Tinsley: 5187SA and Dafang: WZPB-1) with an uncertainty of ±2 mK, a precision thermometer bridge (Tinsley: 5840D) with an uncertainty of ±1 mK to provide a more precise temperature measurement in the constant temperature period, a selector switch (Tinsley: 5840CS/6T), a personal computer, and a super thermometer (HART: 1590) to supervise the temperature increasing process. The overall temperature uncertainty including the bath temperature variation and the temperature measurement system was less than ±10 mK. The temperature was determined on the basis of the International Temperature Scale of 1990 (ITS-90).

The pressure measurement system, which could measure pressures up to 6 MPa, included a piston-type pressure gauge, a pressure transducer, and two digital manometers. A highly sensitive diaphragm pressure transducer (Rousemount: 3051S) with an uncertainty of ±0.1 % separated the sample in the thermostat bath from nitrogen that transmitted the pressure to outside the bath. An absolute pressure digital manometer (Yokogawa: MT210) was used to measure the atmospheric pressure with an uncertainty of ±0.015 % in the range of (0.001 to 130) kPa. The pressures in these experiments varied from (105 to 3658) kPa. At pressures below 130 kPa, the nitrogen transmitted the sample pressure directly to the absolute pressure digital manometer. Pressures above 0.13 MPa and below 3 MPa were measured with a gauge pressure digital manometer (Yokogawa: MT210) with an uncertainty of ±0.015 % in the range of (−0.08 to 3) MPa gauge pressure with the atmospheric pressure then measured with an absolute pressure digital manometer. Two sets of digital pressure manometers were used to measure the pressure in parallel to avoid systemic errors. The pressure measurement system had a maximum uncertainty of ±100 Pa.

The highest vacuum provided by the turbo-molecular pump (KYKY FD110) was about $1 \cdot 10^{-6}$ Pa.

Before the experiments, the platinum resistance thermometers, the thermometer bridge with the selector switch, the super thermometer, and the digital manometers were calibrated by the National Institute of Metrology, China. Before and after use, the sensitive diaphragm pressure transducer was tested using the digital manometers. The zero of the sensitive diaphragm pressure transducer varied as the pressure and temperature changed, thus a corrected function for the zero was derived to provide more accurate pressure data.

The Burnett apparatus including the two cells was made of 1Cr18Ni9Ti stainless steel. The inside of the sample cell, B2, with a volume of 500 mL and the expansion cell, B1, with a volume of 200 mL was polished to reduce the effect of physical adsorption. Before the experiments, the two cells were rinsed with acetone to remove any residue from previous experiments.

The HFC-32 sample was obtained from Zhejiang Fluoro-Chemical Technology Research Institute and was used without

* Corresponding author. Telephone: +86-10-6279-6318. Fax: +86-10-6277-0209. E-mail address: yyduan@mail.tsinghua.edu.cn.

10.1021/je7000667 CCC: $37.00

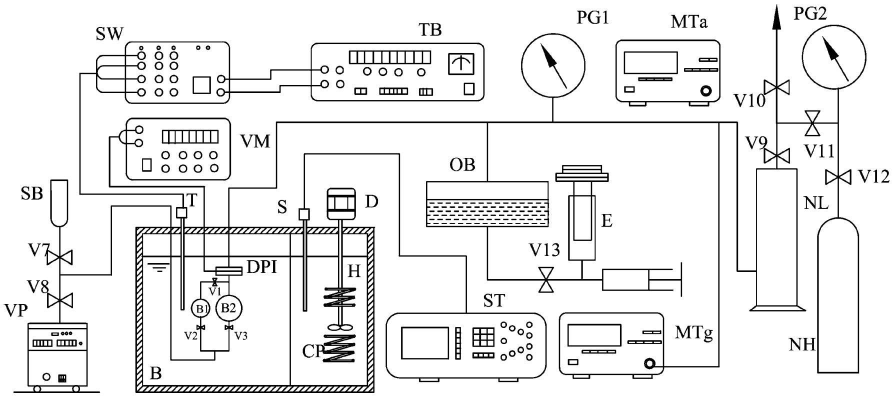

Figure 1. Burnett experimental apparatus: B, thermostatic bath; B1, expansion cell (200 mL); B2, sample cell (500 mL); ST, super thermometer; CP, cooler; D, stirrer; DPI, differential pressure detector; E, oil piston-type pressure gauge; H, heater; NH, N_2 bottle; NL, pressure damper; OB, oil−gas separator; PG1, PG2, pressure gauges; T, platinum resistance thermometer; S, temperature sensor; SB, sample bottle; SW, selector switch; TB, thermometer bridge; V1∼V13, valves; VM, digital multimeter; VP, vacuum pump; MTa, absolute pressure digital manometer; MTg, gauge pressure digital manometer.

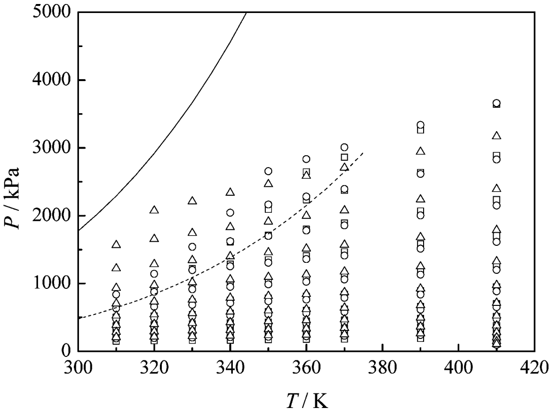

Figure 2. Distribution of experimental HFC-32 (1) + HFC-227ea (2) data: □, $x_1 = 0.2648$; ○, $x_1 = 0.5155$; △, $x_1 = 0.7809$; —, vapor pressures for HFC-32;[7] ----, vapor pressures for HFC-227ea.[8]

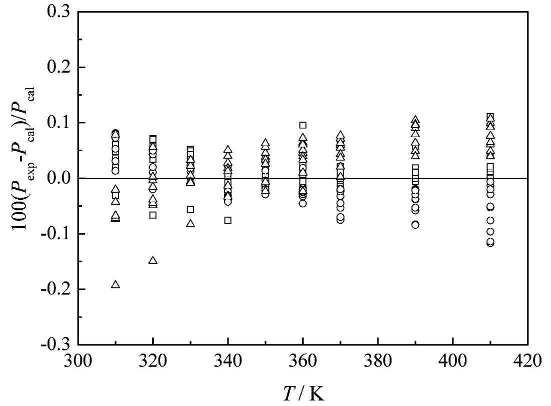

Figure 3. Pressure deviations of experimental *PVTx* data from calculated results for HFC-32 (1) + HFC-227ea (2) mixtures: □, $x_1 = 0.2648$; ○, $x_1 = 0.5155$; △, $x_1 = 0.7809$.

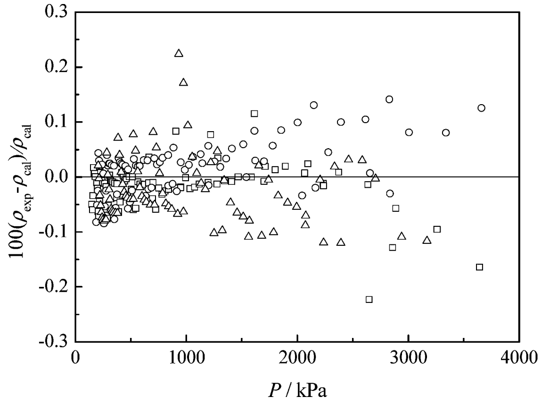

Figure 4. Density deviations of experimental *PVTx* data from calculated results for HFC-32 (1) + HFC-227ea (2) mixtures: □, $x_1 = 0.2648$; ○, $x_1 = 0.5155$; △, $x_1 = 0.7809$.

further purification, with a stated purity of mass fraction more than 99.95 %. The HFC-227ea sample was obtained from Shanghai Huiyou Chemical Corp. and was used without further purification, with a stated purity of mole fraction better than 99.9 % and water content less than 20 ppm. Before use, the HFC-32 and HFC-227ea samples in the sample bottles were frozen with liquefied nitrogen and the vapor space was evacuated by a vacuum pump (KYKY FD110) to remove possible air impurities. A gas chromatograph (Lunan SP-6800A) with a thermal conductivity detector (TCD) and an ODPN (*β*,*β*-oxydipropionitrile) column was used to examine the deaerated samples, and the impurities were found to be less than 0.03 % for both samples on the basis of the area response of the TCD.

The cell constant, N_0, defined as the ratio of the sum of the volumes of cells B1 and B2 to the volume of cell B2 at vacuum, was determined by measurements with gaseous helium. The N used in the data processing is not dependent on temperature, but is a weak function of pressure

$$N(P_{i-1},P_i) = N_0 \frac{1 + mP_i}{1 + mP_{i-1}} \tag{1}$$

where the coefficient m should be a constant, found to be $4.0135 \cdot 10^{-11}$ Pa^{-1} in this work. Two series of expansion data for helium at 318.15 K yielded the cell constant $N_0 = 1.379\,69 \pm 0.000\,01$.

Compared to the *PVT* measurements of pure refrigerants, a key process in *PVTx* measurements is to prepare mixtures with precise mole fractions and purities. The masses of HFC-32 and HFC-227ea introduced into sample cell B2 were determined by measuring the weight changes of cylinders containing each component using an accurate electronic balance (Mettler Toledo: PR1203) with a resolution of ±0.001 g. Three HFC-32 (1) + HFC-227ea (2) binary mixtures were prepared with x_1 mole fractions of 0.2648, 0.5155, and 0.7809. Before the two components were introduced into the sample cell, they were frozen with liquefied nitrogen, and the vapor space was evacuated by the vacuum pump to 10^{-4} Pa to remove possible air impurities. Two Burnett cells and the connections were then evacuated by the vacuum pump to remove impurities. The vacuum in the system was better than $5 \cdot 10^{-5}$ Pa and was

Table 1. Experimental *PVTx* Properties of HFC-32 (1) + HFC-227ea (2) Mixtures

T	P	ρ			T	P	ρ			T	P	ρ		
K	kPa	$\text{kg}\cdot\text{m}^{-3}$	Z	x_1	K	kPa	$\text{kg}\cdot\text{m}^{-3}$	Z	x_1	K	kPa	$\text{kg}\cdot\text{m}^{-3}$	Z	x_1
410.00	3641.58	206.107	0.71930	0.2648	330.00	159.77	8.281	0.97583	0.2648	340.00	388.85	15.688	0.95745	0.5155
410.00	2887.09	149.389	0.78678	0.2648	320.00	904.50	57.140	0.82569	0.2648	340.00	285.24	11.372	0.96891	0.5155
410.00	2234.99	108.280	0.84032	0.2648	320.00	693.04	41.416	0.87284	0.2648	340.00	208.54	8.243	0.97727	0.5155
410.00	1699.56	78.483	0.88161	0.2648	320.00	522.08	30.019	0.90716	0.2648	330.00	1539.99	78.443	0.78132	0.5155
410.00	1275.55	56.886	0.91287	0.2648	320.00	388.88	21.758	0.93226	0.2648	330.00	1198.36	56.859	0.83879	0.5155
410.00	948.18	41.232	0.93621	0.2648	320.00	287.44	15.771	0.95069	0.2648	330.00	913.06	41.214	0.88169	0.5155
410.00	699.84	29.885	0.95335	0.2648	320.00	211.27	11.431	0.96404	0.2648	330.00	685.57	29.874	0.91332	0.5155
410.00	513.94	21.661	0.96592	0.2648	320.00	154.66	8.285	0.97365	0.2648	330.00	509.64	21.654	0.93668	0.5155
410.00	376.14	15.701	0.97531	0.2648	310.00	662.59	41.446	0.86079	0.2648	330.00	376.17	15.696	0.95381	0.5155
410.00	274.54	11.380	0.98214	0.2648	310.00	501.26	30.041	0.89843	0.2648	330.00	276.22	11.377	0.96623	0.5155
410.00	199.99	8.248	0.98710	0.2648	310.00	374.40	21.774	0.92583	0.2648	330.00	202.10	8.247	0.97531	0.5155
410.00	145.48	5.979	0.99062	0.2648	310.00	277.27	15.782	0.94595	0.2648	320.00	1142.48	56.888	0.82426	0.5155
410.00	105.73	4.333	0.99329	0.2648	310.00	204.07	11.439	0.96053	0.2648	320.00	875.19	41.235	0.87110	0.5155
390.00	3260.41	206.316	0.67635	0.2648	310.00	149.52	8.291	0.97099	0.2648	320.00	659.50	29.889	0.90559	0.5155
390.00	2633.96	149.541	0.75385	0.2648	410.00	3658.20	148.709	0.78800	0.5155	320.00	491.50	21.665	0.93109	0.5155
390.00	2065.64	108.390	0.81564	0.2648	410.00	2827.96	107.791	0.84040	0.5155	320.00	363.38	15.704	0.94970	0.5155
390.00	1584.77	78.563	0.86334	0.2648	410.00	2149.18	78.132	0.88113	0.5155	320.00	267.14	11.383	0.96320	0.5155
390.00	1196.66	56.943	0.89942	0.2648	410.00	1613.03	56.634	0.91235	0.5155	320.00	195.61	8.251	0.97303	0.5155
390.00	893.34	41.274	0.92636	0.2648	410.00	1199.10	41.051	0.93568	0.5155	310.00	836.50	41.255	0.85902	0.5155
390.00	661.34	29.916	0.94615	0.2648	410.00	885.10	29.756	0.95283	0.5155	310.00	633.01	29.904	0.89681	0.5155
390.00	486.71	21.683	0.96066	0.2648	410.00	650.20	21.568	0.96566	0.5155	310.00	473.07	21.676	0.92463	0.5155
390.00	356.74	15.716	0.97148	0.2648	410.00	475.89	15.634	0.97507	0.5155	310.00	350.46	15.712	0.94500	0.5155
390.00	260.65	11.392	0.97929	0.2648	410.00	347.32	11.332	0.98177	0.5155	310.00	258.01	11.389	0.95982	0.5155
390.00	190.02	8.257	0.98498	0.2648	410.00	253.05	8.214	0.98683	0.5155	310.00	189.10	8.255	0.97052	0.5155
370.00	2859.18	206.516	0.62458	0.2648	410.00	184.04	5.954	0.99013	0.5155	410.00	3168.33	84.141	0.86026	0.7809
370.00	2371.09	149.686	0.71460	0.2648	410.00	133.75	4.316	0.99277	0.5155	410.00	2392.39	60.988	0.89617	0.7809
370.00	1891.19	108.495	0.78636	0.2648	390.00	3338.36	148.860	0.75522	0.5155	410.00	1786.74	44.206	0.92339	0.7809
370.00	1467.26	78.639	0.84172	0.2648	390.00	2613.57	107.901	0.81569	0.5155	410.00	1325.09	32.073	0.94387	0.7809
370.00	1116.32	56.999	0.88353	0.2648	390.00	2003.73	78.212	0.86274	0.5155	410.00	975.71	23.247	0.95885	0.7809
370.00	837.70	41.314	0.91473	0.2648	390.00	1513.03	56.692	0.89876	0.5155	410.00	715.45	16.850	0.97001	0.7809
370.00	622.40	29.945	0.93767	0.2648	390.00	1129.55	41.093	0.92567	0.5155	410.00	522.95	12.214	0.97818	0.7809
370.00	459.23	21.704	0.95450	0.2648	390.00	836.32	29.786	0.94553	0.5155	410.00	381.49	8.853	0.98448	0.7809
370.00	337.19	15.732	0.96694	0.2648	390.00	615.63	21.590	0.96023	0.5155	410.00	277.79	6.417	0.98902	0.7809
370.00	246.70	11.403	0.97601	0.2648	390.00	451.27	15.650	0.97105	0.5155	410.00	201.86	4.651	0.99156	0.7809
370.00	180.00	8.265	0.98249	0.2648	390.00	329.74	11.344	0.97888	0.5155	410.00	146.65	3.371	0.99381	0.7809
360.00	2647.82	206.618	0.59418	0.2648	390.00	240.40	8.222	0.98458	0.5155	410.00	106.47	2.443	0.99548	0.7809
360.00	2234.41	149.760	0.69177	0.2648	370.00	3006.52	149.004	0.71621	0.5155	390.00	2940.03	84.226	0.83835	0.7809
360.00	1801.25	108.549	0.76939	0.2648	370.00	2392.59	108.005	0.78632	0.5155	390.00	2236.42	61.050	0.87982	0.7809
360.00	1407.12	78.678	0.82923	0.2648	370.00	1854.71	78.287	0.84093	0.5155	390.00	1679.09	44.251	0.91133	0.7809
360.00	1075.41	57.027	0.87436	0.2648	370.00	1411.02	56.746	0.88262	0.5155	390.00	1249.85	32.105	0.93498	0.7809
360.00	809.48	41.334	0.90802	0.2648	370.00	1058.90	41.133	0.91379	0.5155	390.00	922.76	23.271	0.95234	0.7809
360.00	602.72	29.960	0.93278	0.2648	370.00	786.90	29.815	0.93684	0.5155	390.00	677.89	16.867	0.96523	0.7809
360.00	445.38	21.715	0.95096	0.2648	370.00	580.80	21.611	0.95395	0.5155	390.00	496.17	12.226	0.97470	0.7809
360.00	327.36	15.740	0.96434	0.2648	370.00	426.48	15.665	0.96638	0.5155	390.00	362.31	8.862	0.98194	0.7809
360.00	239.67	11.408	0.97408	0.2648	370.00	312.04	11.355	0.97547	0.5155	390.00	264.02	6.423	0.98720	0.7809
360.00	174.96	8.269	0.98106	0.2648	370.00	227.73	8.230	0.98215	0.5155	370.00	2705.17	84.308	0.81229	0.7809
350.00	2092.92	149.834	0.66615	0.2648	360.00	2834.79	149.078	0.69372	0.5155	370.00	2076.94	61.109	0.86041	0.7809
350.00	1709.09	108.602	0.75051	0.2648	360.00	2279.03	108.059	0.76943	0.5155	370.00	1569.39	44.294	0.89696	0.7809
350.00	1345.81	78.717	0.81536	0.2648	360.00	1778.47	78.326	0.82835	0.5155	370.00	1172.78	32.136	0.92386	0.7809
350.00	1033.94	57.055	0.86423	0.2648	360.00	1359.13	56.775	0.87334	0.5155	370.00	869.16	23.293	0.94461	0.7809
350.00	780.99	41.355	0.90065	0.2648	360.00	1023.13	41.153	0.90700	0.5155	370.00	639.98	16.884	0.95958	0.7809
350.00	582.86	29.974	0.92735	0.2648	360.00	761.94	29.830	0.93186	0.5155	370.00	469.20	12.238	0.97060	0.7809
350.00	431.39	21.726	0.94695	0.2648	360.00	563.21	21.622	0.95028	0.5155	370.00	343.02	8.870	0.97896	0.7809
350.00	317.47	15.747	0.96146	0.2648	360.00	414.00	15.673	0.96368	0.5155	370.00	250.16	6.429	0.98501	0.7809
350.00	232.62	11.414	0.97196	0.2648	360.00	303.15	11.360	0.97352	0.5155	360.00	2584.71	84.349	0.79729	0.7809
350.00	169.93	8.273	0.97956	0.2648	360.00	221.36	8.234	0.98073	0.5155	360.00	1995.52	61.139	0.84922	0.7809
340.00	1614.05	108.656	0.72926	0.2648	350.00	2654.54	149.152	0.66784	0.5155	360.00	1513.67	44.316	0.88870	0.7809
340.00	1283.14	78.756	0.79985	0.2648	350.00	2162.67	108.113	0.75063	0.5155	360.00	1134.08	32.152	0.91773	0.7809
340.00	991.76	57.084	0.85294	0.2648	350.00	1700.78	78.365	0.81440	0.5155	360.00	842.09	23.305	0.94014	0.7809
340.00	752.13	41.375	0.89242	0.2648	350.00	1306.47	56.803	0.86306	0.5155	360.00	620.87	16.892	0.95631	0.7809
340.00	562.85	29.989	0.92139	0.2648	350.00	986.94	41.173	0.89946	0.5155	360.00	455.62	12.244	0.96821	0.7809
340.00	417.35	21.737	0.94259	0.2648	350.00	736.76	29.844	0.92634	0.5155	360.00	333.32	8.875	0.97722	0.7809
340.00	307.52	15.755	0.95825	0.2648	350.00	545.49	21.633	0.94622	0.5155	360.00	243.21	6.433	0.98372	0.7809
340.00	225.54	11.420	0.96960	0.2648	350.00	401.46	15.680	0.96072	0.5155	350.00	2461.96	84.391	0.78073	0.7809
340.00	164.86	8.277	0.97781	0.2648	350.00	294.24	11.366	0.97142	0.5155	350.00	1912.81	61.169	0.83687	0.7809
330.00	1218.71	78.795	0.78232	0.2648	350.00	214.96	8.239	0.97909	0.5155	350.00	1457.22	44.338	0.87957	0.7809
330.00	948.75	57.112	0.84026	0.2648	340.00	2042.81	108.166	0.72952	0.5155	350.00	1094.95	32.168	0.91093	0.7809
330.00	722.83	41.396	0.88322	0.2648	340.00	1621.43	78.404	0.79884	0.5155	350.00	814.82	23.317	0.93522	0.7809
330.00	542.59	30.004	0.91470	0.2648	340.00	1252.91	56.831	0.85160	0.5155	350.00	601.65	16.901	0.95271	0.7809
330.00	403.18	21.748	0.93772	0.2648	340.00	950.24	41.194	0.89105	0.5155	350.00	441.97	12.250	0.96555	0.7809
330.00	297.52	15.763	0.95468	0.2648	340.00	711.31	29.859	0.92019	0.5155	350.00	323.59	8.879	0.97530	0.7809
330.00	218.42	11.425	0.96695	0.2648	340.00	527.64	21.643	0.94171	0.5155	350.00	236.22	6.436	0.98227	0.7809
340.00	2336.21	84.433	0.76226	0.7809	330.00	1015.20	32.200	0.89487	0.7809	320.00	400.53	12.268	0.95562	0.7809
340.00	1828.54	61.200	0.82312	0.7809	330.00	759.44	23.340	0.92357	0.7809	320.00	294.06	8.892	0.96796	0.7809
340.00	1399.94	44.360	0.86942	0.7809	330.00	562.74	16.917	0.94417	0.7809	320.00	215.08	6.445	0.97678	0.7809

Table 1 (Continued)

T	P	ρ			T	P	ρ			T	P	ρ		
K	kPa	$kg \cdot m^{-3}$	Z	x_1	K	kPa	$kg \cdot m^{-3}$	Z	x_1	K	kPa	$kg \cdot m^{-3}$	Z	x_1
340.00	1055.37	32.184	0.90337	0.7809	330.00	414.44	12.262	0.95932	0.7809	310.00	1562.63	61.291	0.77034	0.7809
340.00	787.28	23.328	0.92973	0.7809	330.00	303.95	8.888	0.97069	0.7809	310.00	1221.26	44.426	0.83061	0.7809
340.00	582.27	16.909	0.94868	0.7809	330.00	222.17	6.442	0.97886	0.7809	310.00	932.70	32.232	0.87433	0.7809
340.00	428.24	12.256	0.96260	0.7809	320.00	2072.72	84.517	0.71785	0.7809	310.00	702.73	23.363	0.90883	0.7809
340.00	313.78	8.884	0.97309	0.7809	320.00	1653.92	61.261	0.79026	0.7809	310.00	523.12	16.934	0.93339	0.7809
340.00	229.21	6.439	0.98066	0.7809	320.00	1282.18	44.404	0.84521	0.7809	310.00	386.48	12.274	0.95139	0.7809
330.00	2206.83	84.475	0.74150	0.7809	320.00	974.36	32.216	0.88528	0.7809	310.00	284.06	8.897	0.96473	0.7809
330.00	1742.40	61.230	0.80771	0.7809	320.00	731.28	23.351	0.91666	0.7809	310.00	207.98	6.449	0.97449	0.7809
330.00	1341.66	44.382	0.85805	0.7809	320.00	543.05	16.926	0.93913	0.7809					

Table 2. Numerical Constants in Equations 6 and 7 for HFC-32 (1) + HFC-227ea (2) Mixtures

	$B_{0,ij}$	$B_{1,ij}$	$B_{2,ij}$	$B_{3,ij}$	$B_{4,ij}$	$B_{5,ij}$
ij	$cm^3 \cdot mol^{-1}$	$cm^3 \cdot mol^{-1}$	$cm^3 \cdot mol^{-1}$	$cm^3 \cdot mol^{-1}$	$cm^3 \cdot mol^{-1}$	$cm^3 \cdot mol^{-1}$
11	−0.1209454	0.608827	−1.022743	0.364650	−0.022173	−0.0034218
22	1.415035	−4.844988	5.745951	−2.837906	0.180537	−0.0214747
12	55.45962	−226.7051	327.9155	−173.3372	20.69367	−4.241273

	$C_{0,ijk}$	$C_{1,ijk}$	$C_{2,ijk}$	$C_{3,ijk}$
ijk	$cm^6 \cdot mol^{-2}$	$cm^6 \cdot mol^{-2}$	$cm^6 \cdot mol^{-2}$	$cm^6 \cdot mol^{-2}$
111	1.175230	−3.304421	2.591649	−0.444488
222	6.442379	−17.768316	13.768861	−2.397078
112	14.248403	−39.160429	30.245157	−5.312519
122	−7.835912	20.946128	−15.766611	2.672564

Table 3. Deviations of the Experimental *PVTx* Data from the Present Virial EOS for HFC-32 (1) + HFC-227ea (2) Mixtures

$100 \cdot \delta_{max}(P)$[a]	$100 \cdot \delta_{rms}(P)$[b]	$100 \cdot \delta_{max}(\rho)$[c]	$100 \cdot \delta_{rms}(\rho)$[d]
0.193	0.047	0.234	0.056

[a] $\delta_{max}(P) = \max(P_{i,exptl}/P_{i,calcd} - 1)$.

[b] $\delta_{rms}(P) = \sqrt{\sum_{i=1}^{n} (P_{i,exptl}/P_{i,calcd} - 1)^2/(n - 1)}$.

[c] $\delta_{max}(\rho) = \max(\rho_{i,exptl}/\rho_{i,calcd} - 1)$.

[d] $\delta_{rms}(\rho) = \sqrt{\sum_{i=1}^{n} (\rho_{i,exptl}/\rho_{i,calcd} - 1)^2/(n - 1)}$.

maintained for at least 5 h. Because the vapor pressure of HFC-227ea is lower than that of HFC-32 at the same temperature, a designed amount of HFC-227ea was first introduced into cell B2 from the gas cylinder. Then the valve was closed, and the cylinder was cooled by liquefied nitrogen to force the HFC-227ea vapor in the pipeline back into the gas cylinder. After cell B2 was cooled by frozen ice, the designed mass of HFC-32 was added to cell B2 from the other gas cylinder using the same procedure. After introducing the HFC-32 to the sample cell, the cylinder filled with the residual HFC-32 was connected to the gas chromatograph to check whether the HFC-227ea returned to the cylinder. Because the sample mass introduced to cell B2 was about 50 g, the uncertainty of the calculated mixture's composition was estimated to be less than ±0.01 % mole fraction.

After the sample cell was filled, the temperatures and pressures were accurately measured for various processes. REFPROP (ver. 7.1) was used to verify that these initial conditions were indeed in the gaseous phase for the mixture. Then the thermostat bath temperature was controlled to the decided temperature. The sample was assumed to be in thermal equilibrium with the bath fluid when more than three pressure measurements measured every 10 min had differences of less than ±50 Pa. The sample temperature and pressure were then measured. When a series of pressure measurements at temperature intervals of 10 K were completed, valve V1 was opened and the working fluid was expanded into cell B1 at 410 K. Before the expansion, cell B1 was evacuated to less than $5 \cdot 10^{-5}$ Pa with valve V2 open and V1 and V3 closed. Then V2 was closed and V1 was opened to expand part of the sample fluid into the expansion cell in the single phase. Valve V1 was kept open for at least 30 min to ensure uniform density and to promote homogeneity of the sample. During the expansion, the temperature was stable at the highest experimental temperature to ensure that the mixture was in the vapor phase. The constant temperature was used to make sure that the mixture was distributed uniformly in the sample and expansion cells. The temperature and pressure were then measured to compare with the measurements of the next day to verify that the system was sealed. Then the apparatus was cooled along the isochore with the *PVTx* measurements, and the isothermal expansion procedure was repeated for several isochores. The mixture composition was verified after each expansion by measuring the sample in the expansion cell with the gas chromatograph. The detector response was carefully calibrated using gravimetrically prepared mixtures so that the gas chromatograph reproducibility for each sample was within ±0.1 %.

Results and Discussion

The density values can be calculated in two ways. The first is to use

$$\rho_i = \frac{P_i}{Z_i RT} = \frac{1}{N^i ART} \tag{2}$$

where ρ_i denotes the molar density; P_i is the pressure; Z_i is the compressibility factor; R is the universal gas constant; T is the temperature; N is the cell constant; and A is the gas-filled constant. The second method uses data along an isochore starting with the density at the highest temperature (410 K) determined from eq 2 for each Burnett expansion step combined with the calculated thermal expansion characteristics of the cell with

Table 4. Second and Third Virial Coefficients for HFC-32 (1) + HFC-227ea (2) Mixtures

T	B_m	C_m	T	B_m	C_m
K	$cm^3 \cdot mol^{-1}$	$cm^6 \cdot mol^{-2}$	K	$cm^3 \cdot mol^{-1}$	$cm^6 \cdot mol^{-2}$
		$x_1 = 0.2648$			
310.00	−466.4	14 797	360.00	−318.6	30 619
320.00	−428.0	16 968	370.00	−295.6	28 803
330.00	−397.4	26 208	390.00	−255.5	25 147
340.00	−368.9	29 567	410.00	−221.5	21 795
350.00	−342.5	30 667			
		$x_1 = 0.5155$			
310.00	−375.6	17 480	360.00	−255.5	22 753
320.00	−346.3	21 198	370.00	−236.9	21 168
330.00	−320.6	23 770	390.00	−204.6	18 319
340.00	−297.8	25 093	410.00	−177.3	15 817
350.00	−275.0	23 407			
		$x_1 = 0.7809$			
310.00	−315.8	29 930	360.00	−207.0	18 245
320.00	−287.9	25 877	370.00	−191.7	16 857
330.00	−264.0	23 771	390.00	−162.9	12 430
340.00	−242.8	21 735	410.00	−140.9	10 712
350.00	−224.1	20 014			

temperature. Because the direct method to obtain the densities using eq 2 may be affected by adsorption, the densities used here were calculated using the second method.

A total of 251 *PVTx* data points for the binary HFC-32 (1) + HFC-227ea (2) mixture were obtained in the gaseous phase with temperatures from (310 to 410) K, pressures up to 3658 kPa, and three different mixture compositions of $x_1 = 0.2648$ ($w_1 = 0.0993$), $x_1 = 0.5155$ ($w_1 = 0.2456$), and $x_1 = 0.7809$ ($w_1 = 0.5216$). The corresponding temperature (T/K), pressure (P/kPa), density ($\rho/\mathrm{kg \cdot m^{-3}}$), compressibility factor (Z), and HFC-32 mole fraction (x_1) data are listed in Table 1. The relative expanded uncertainties for density and compressibility factor are ±0.05 % and ±0.06 % with a level of confidence of 95 %. Figure 2 illustrates the *PVTx* data distribution, where the vapor pressure curve of HFC-32 was calculated from that of Tillner−Roth and Yokozeki[7] and the vapor pressure curve of HFC-227ea was from the equation of state of Wang and Duan.[8]

A truncated virial EOS for the HFC-32 + HFC-227ea system was developed by fitting the data listed in Table 1. The equation was based on the following functional form

$$Z = \frac{P}{\rho RT} = 1 + B_m \rho + C_m \rho^2 \tag{3}$$

where B_m and C_m denote the second and third mixture virial coefficients given by

$$B_m = \sum_i^2 \sum_j^2 x_i x_j B_{ij} \tag{4}$$

$$C_m = \sum_i^2 \sum_j^2 \sum_k^2 x_i x_j x_k C_{ijk} \tag{5}$$

Note that if $i = j = k$, B_{ij} and C_{ijk} correspond to the virial coefficients for the pure component. The *PVT* data of the pure HFC-32 and HFC-227ea components were obtained from Tillner−Roth and Yokozeki[7] and Dong et al.[9] to calculate B_{11}, C_{111}, B_{22}, and C_{222}. Both B_{ij} and C_{ijk} were expressed as functions of the reduced temperature, $T_{r,ij(k)} = T/T_{C,ij(k)}$, as

$$B_{ij} = B_{0,ij} + B_{1,ij}T_{r,ij}^{-1} + B_{2,ij}T_{r,ij}^{-2} + B_{3,ij}T_{r,ij}^{-3} + B_{4,ij}T_{r,ij}^{-6} + B_{5,ij}T_{r,ij}^{-8} \tag{6}$$

$$C_{ijk} = C_{0,ijk} + C_{1,ijk}T_{r,ijk}^{-0.5} + C_{2,ijk}T_{r,ijk}^{-1} + C_{3,ijk}T_{r,ijk}^{-2} \tag{7}$$

The characteristic temperature, $T_{C,ij(k)}$, was defined for the cross second and third virial coefficients of the mixture as

$$T_{C,ij} = \sqrt{T_{C,i}T_{C,j}} \tag{8}$$

$$T_{C,ijk} = \sqrt[3]{T_{C,i}T_{C,j}T_{C,k}} \tag{9}$$

The critical temperature of HFC-32 used was 351.255 K,[10] and that of HFC-227ea was 375.95 K.[11] The coefficients in eqs 4 and 5 for the HFC-32 + HFC-227ea mixtures are listed in Table 2. Several data points at 410 K at low pressure were unreasonable, so a total of 244 sets of data were used for the fitting process.

Figure 3 shows the relative pressure deviation distribution of the experimental data from eqs 3 to 7. The data can be well represented by the truncated virial equation within ±0.193 % over the entire range. The deviations of the density measurements from the present virial EOS are also shown in Figure 4, within a maximum deviation of 0.224 %. The detailed maximum and root mean square (rms) deviations are listed in Table 3.

The experimental second and third coefficients, $B_m(T)$ and $C_m(T)$, were obtained by fitting eq 3 to the experimental data, with the results listed in Table 4. The cross second and third virial coefficients were listed in Table 5.

Figures 5 and 6 show the temperature dependence of the experimental and calculated B_m and C_m for the three mixture compositions along with the virial coefficients of the pure components. The estimated expanded uncertainties are ±1 $cm^3 \cdot mol^{-1}$ for B_m and ±500 $cm^6 \cdot mol^{-2}$ for C_m. The calculated virial coefficients are in good agreement with the experimental data at higher temperatures, with a somewhat larger deviation

Table 5. Cross Second and Third Virial Coefficients for HFC-32 (1) + HFC-227ea (2) Mixtures[a]

T	B_{11}	B_{12}	B_{22}	C_{111}	C_{112}	C_{122}	C_{222}
K	$cm^3 \cdot mol^{-1}$	$cm^3 \cdot mol^{-1}$	$cm^3 \cdot mol^{-1}$	$cm^6 \cdot mol^{-2}$	$cm^6 \cdot mol^{-2}$	$cm^6 \cdot mol^{-2}$	$cm^6 \cdot mol^{-2}$
310.00	−269.9	−333.2	−597.8	23 679	7434	35 120	47 690
320.00	−248.7	−305.3	−551.3	22 418	15 002	28 957	50 940
330.00	−229.8	−282.2	−509.4	21 037	19 241	24 536	52 282
340.00	−212.9	−260.7	−471.6	19 599	21 100	21 363	52 221
350.00	−197.6	−240.2	−437.5	18 151	21 334	19 048	51 161
360.00	−183.8	−221.0	−406.5	16 729	20 535	17 283	49 420
370.00	−171.2	−203.2	−378.4	15 361	19 171	15 826	47 253
390.00	−149.1	−172.7	−329.3	12 863	16 142	13 117	42 410
410.00	−130.5	−146.4	−287.8	10 763	14 315	9852	37 785

[a] The second and third virial coefficients of pure HFC-32 were obtained from Tillner−Roth and Yokozeki,[7] and those of HFC-227ea were obtained from Dong et al.[9]

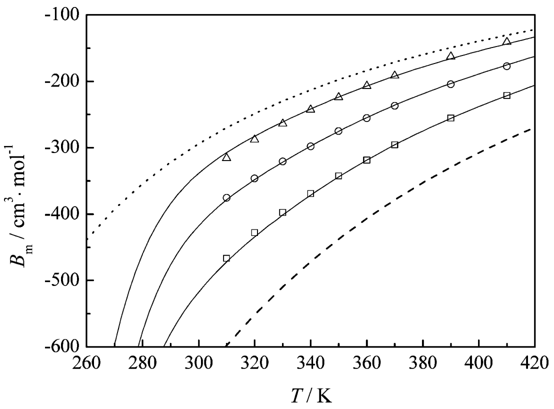

Figure 5. Temperature dependence of the second virial coefficients for HFC-32 (1) + HFC-227ea (2) mixtures: □, $x_1 = 0.2648$; ○, $x_1 = 0.5155$; △, $x_1 = 0.7809$; —, eq 4; ···, the second virial coefficient of HFC-32;[7] ---, the second virial coefficient of HFC-227ea.[9]

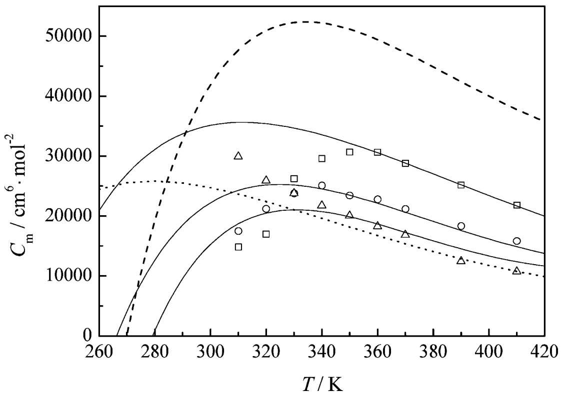

Figure 6. Temperature dependence of the third virial coefficients for HFC-32 (1) + HFC-227ea (2) mixtures: □, $x_1 = 0.2648$; ○, $x_1 = 0.5155$; △, $x_1 = 0.7809$; —, eq 5; ···, third virial coefficient of HFC-32;[7] ---, third virial coefficient of HFC-227ea.[9]

at lower temperatures. The differences are obvious in Figure 6, which presents the C_m values. One reason may be the uncertainty in the mixture mole fraction, even with extremely careful experimental measurements. The absolute uncertainty of the gas chromatograph measurement was ±0.1 %, but the mixture mole fraction may have varied a small amount during the repeated Burnett expansions.

Conclusions

A total of 251 *PVTx* data points were measured in the gaseous phase for HFC-32 (1) + HFC-227ea (2) mixtures using the Burnett-isochoric method for three different compositions ($x_1 = 0.2648$, $x_1 = 0.5155$, and $x_1 = 0.7809$) with temperatures from (310 to 410) K and pressures up to 3658 kPa. The temperature and pressure measurement uncertainties were less than ±10 mK and ±100 Pa. A truncated virial EOS was used to fit the experimental data to facilitate calculation of the thermophysical properties. The calculated virial coefficients, B_m and C_m, agreed well with the experimental values except in the low-temperature range.

Literature Cited

(1) Lin, H.; Duan, Y. Y. Surface Tension of Difluoromethane (R-32) + 1,1,1,2,3,3,3-Heptafluoropropane (R-227ea) from (253 to 333) K. *J. Chem. Eng. Data* **2005**, *50*, 182−186.

(2) Coquelet, C.; Hong, D. N.; Chareton, A.; Baba-Agmed, A.; Richon, D. Vapour−Liquid Equilibrium Data for the Difluoromethane + 1,1,1,2,3,3,3-Heptafluoropropane System at Temperatures from 283.20 to 343.38 K and Pressure up to 4.5 MPa. *Int. J. Refrig.* **2003**, *26*, 559−565.

(3) Park, J. Y.; Lim, J. S.; Lee, B. G.; Lee, Y. W. Phase Equilibria of CFC Alternative Refrigerant Mixtures: 1,1,1,2,3,3,3-Heptafluoropropane (HFC-227ea) + Difluoromethane (HFC-32), + 1,1,1,2-Tetrafluoroethane (HFC-134a), and + 1,1-Difluoroethane (HFC-152a). *Int. J. Thermophys.* **2001**, *22*, 901−917.

(4) Koo, S.; Chang, J.; Kim, H.; Lee, B. G.; Lee, J. Vapor−liquid Equilibrium Measurements for Binary Mixtures Containing 1,1,1,2,3,3,3-heptafluoropropane (HFC-227ea). *Int. J. Thermophys.* **2000**, *21*, 405−414.

(5) Meng, L.; Duan, Y. Y.; Chen, Q. *PVTx* Properties in the Gas Phase for Difluoromethane (HFC-32) + Pentafluoroethane (HFC-125). *J. Chem. Eng. Data* **2004**, *49*, 1821−1826.

(6) Fu, Y. D.; Han, L. Z.; Zhu, M. S. *PVT* Properties, Vapor Pressure and Critical Parameters of HFC-32. *Fluid Phase Equilib.* **1995**, *111*, 273−286.

(7) Tillner-Roth and Yokozeki, R.; Yokozeki, A. An international standard equation of state for difluoromethane (R-32) for temperatures from the triple point at 136.34 K to 435 K and pressures up to 70 MPa. *J. Phys. Chem. Ref. Data* **1997**, *25* (6), 1273−1328.

(8) Wang, Z. W.; Duan, Y. Y. Vapor Pressures of 1,1,1,3,3-Pentafluoropropane (HFC-245fa) and 1,1,1,2,3,3,3-Heptafluoropropane (HFC-227ea). *J. Chem. Eng. Data* **2004**, *49*, 1581−1585.

(9) Dong, W.; Duan, Y. Y.; Feng, X. J. *PVT* Properties in the Gas Phase for HFC-227ea. *Refrig. J.* **2006**, *27*, 36−39.

(10) Kuwabara, S.; Aoyama, H.; Sato, H.; Watanabe, K. Vapor−liquid coexistence curve in the critical region and the critical temperatures and densities of difluoromethane and pentafluoroethane. *J. Chem. Eng. Data* **1995**, *40* (1), 112−116.

(11) Defibaugh, D. R.; Moldover, M. R. Compressed and Saturated Liquid Densities for 18 Halogenated Organic Compounds. *J. Chem. Eng. Data* **1997**, *42*, 160−168.

Received for review February 3, 2007. Accepted April 2, 2007. This work was supported by the National Natural Science Foundation of China (No. 50636020).

JE7000667